Pergamon

Bioorganic & Medicinal Chemistry 7 (1999) 2343–2352

BIOORGANIC & MEDICINAL CHEMISTRY

Inhibition of Transcription Factor NF-κB by Sesquiterpene Lactones: a Proposed Molecular Mechanism of Action†

Peter Rüngeler,[a,‡] Victor Castro,[b] Gerardo Mora,[b] Nezhun Gören,[c] Walter Vichnewski,[d] Heike L. Pahl,[e] Irmgard Merfort[a,§,*] and Thomas J. Schmidt[f,§]

[a]*Institut für Pharmazeutische Biologie, Universität Freiburg, Schänzlestr. 1, D-79104 Freiburg, Germany*
[b]*Universidad de Costa Rica, Escuela de Quimica and CIPRONA, San José, Costa Rica*
[c]*TUBITAK, Marmara Research Center, Institute for Basic Science, Department of Chemistry, PO Box 21, 41470 Gebze-Kocaeli, Turkey*
[d]*Universidade de Sao Paulo, Faculdade de Ciencias Farmaceuticas de Ribeirao Preto, Via do Cafe, S/N, 14.040-903- Ribeirao Preto-SP, Brazil*
[e]*Department of Experimental Anaesthesiology, University Hospital, Freiburg, Germany*
[f]*Institut für Pharmazeutische Biologie der Heinrich-Heine-Universität Düsseldorf, Universitätsstr. 1, D-40225 Düsseldorf, Germany*

Received 23 February 1999; accepted 6 May 1999

Abstract—Many sesquiterpene lactones (SLs) possess considerable anti-inflammatory activity. They inhibit the transcription factor NF-κB by selectively alkylating its p65 subunit probably by reacting with cysteine residues. Here we assayed 28 sesquiterpene lactones for their ability to inhibit NF-κB. The majority of the potent NF-κB inhibitors possess two reactive centers in form of an α-methylene-γ-lactone group and an α,β- or α,β,γ,δ-unsaturated carbonyl group. Based on computer molecular modelling we propose a molecular mechanism of action, which is able to explain the p65 selectivity of the SLs and the observed correlation of high activity with alkylant bifunctionality. A single bifunctional SL molecule can alkylate the cysteine residue (Cys 38) in the DNA binding loop 1 (L1) *and* a further cysteine (Cys 120) in the nearby E' region. This cross link alters the position of tyrosine 36 and additional amino acids in such a way that their specific interactions with the DNA become impossible. We also created a model for monofunctional SLs.

Introduction

Sesquiterpene lactones (SLs) have been isolated from numerous genera of Compositae.[1] They are described as the active constituents of some medicinal plants such as *Arnica montana* or *Tanacetum parthenium*. SLs are known to possess a wide variety of biological and pharmacological activities. Antimicrobial, antitumoral and anti-inflammatory activities, effects on the central nervous and cardiovascular systems as well as allergenic potency have been described.[2] The activities are mediated chemically by α, β-unsaturated carbonyl structures, such as an α-methylene-γ-lactone, an α,β-unsaturated cyclopentenone or a conjugated ester. These structure elements react with nucleophiles, especially cysteine sulfhydryl groups, by a Michael-type addition.[3,4] Therefore, exposed thiol groups, such as cysteine residues in proteins, appear to be the primary targets of sesquiterpene lactones. The differences in activity between individual SLs may be explained by different numbers of alkylating structural elements.[4–7] However, other factors such as lipophilicity, molecular geometry, and the chemical environment of the target sulfhydryl may also influence the activity of sesquiterpene lactones.[4,7,8]

Several studies have investigated how SLs exert their anti-inflammatory effect. It was shown that SLs modulate many inflammatory processes, for example oxidative phosphorylation, platelet aggregation, histamine

Key words: Sesquiterpene lactones; NF-κB; anti-inflammatory activity; molecular modelling; mechanism of action.
* Corresponding author. Tel.: +49-761-203-2804; fax: +49-761-203-2803; e-mail: merfort@sun2.ruf.uni-freiburg.de
† We dedicate this cooperative work with deep gratitude to our teacher, Professor Dr. Günter Willuhn, Düsseldorf, on the occasion of his 65th birthday.
‡ Part of thesis.
§ These authors contributed equally to the results of this work.

0968-0896/99/$ - see front matter
PII: S0968-0896(99)00195-9

and serotonin release.[9,10] However, despite these results the molecular mechanism by which they exert their anti-inflammatory effect was not sufficiently explained. Recently, we were able to show that nine SLs of the pseudoguaianolide type from flowerheads of *Arnica* species and of the germacranolide type from leaves of *Tithonia diversifolia*, potently inhibit the transcription factor NF-κB at μM concentrations.[11–13]

NF-κB is a central mediator of the human immune response. In the majority of cell types this protein is composed of a p50 and a p65 subunit. It is retained in an inactive cytoplasmic complex by binding to IκB, its inhibitory subunit. A large variety of inflammatory conditions, such as bacterial and viral infections as well as inflammatory cytokines, rapidly induce NF-κB activity. Active NF-κB is released from the cytoplasmic complex by phosphorylation, ubiquitination and degradation of the IκB subunit. The activated factor then translocates to the nucleus where it stimulates the transcription of its target genes. NF-κB regulates the transcription of various inflammatory cytokines, such as IL-1, IL-2, IL-6, IL-8 and TNF-α, as well as genes encoding cyclooxygenase-II, nitric oxide synthase, immunoreceptors, cell adhesion molecules, hematopoetic growth factors and growth factor receptors.[14–16] Pharmacological inhibition of NF-κB in vivo may thus substantially attenuate inflammatory processes.

Comprehensive studies were undertaken with the SL helenalin. We could show that neither IκB degradation nor NF-κB nuclear translocation are inhibited by helenalin. Rather, inhibition of NF-κB is due to direct alkylation of the transcription factor. Helenalin does not modify the p50 subunit, but targets cysteine sulfhydryl groups in the p65 subunit, thus preventing DNA binding of active NF-κB.[11,13] This model is supported by the recent elucidation of the X-ray structure of the p65 homodimer, which shows that cysteine 38 is located within the DNA binding domain and another cysteine, Cys 120, is found in a proximal loop.[17]

Here we investigated 28 sesquiterpene lactones for their ability to inhibit NF-κB activation. These compounds represent all major skeletal classes, including eudesmanolides, guaianolides, pseudoguaianolides and germacranolides. From the latter class, which is divided into subclasses according to the configuration of the double bonds, representatives of the germacrolides, melampolides and heliangolides were chosen. These compounds differ from each other both in their molecular geometry and in the number of alkylating structure elements. To gain information, whether NF-κB inhibition correlates with the lipophilicity of the SLs, we additionally determined the octanol/water partition coefficient (log P) of each compound, from which penetration behavior through biomembranes may be deduced. We investigated the structure–activity relationship of these 28 compounds. Based on these data and on computer molecular modelling we propose a molecular mechanism of action. Two cysteine residues (Cys 38 and Cys 120) in the p65 subunit are targets for alkylation by SLs. Bifunctional compounds can crosslink these two residues

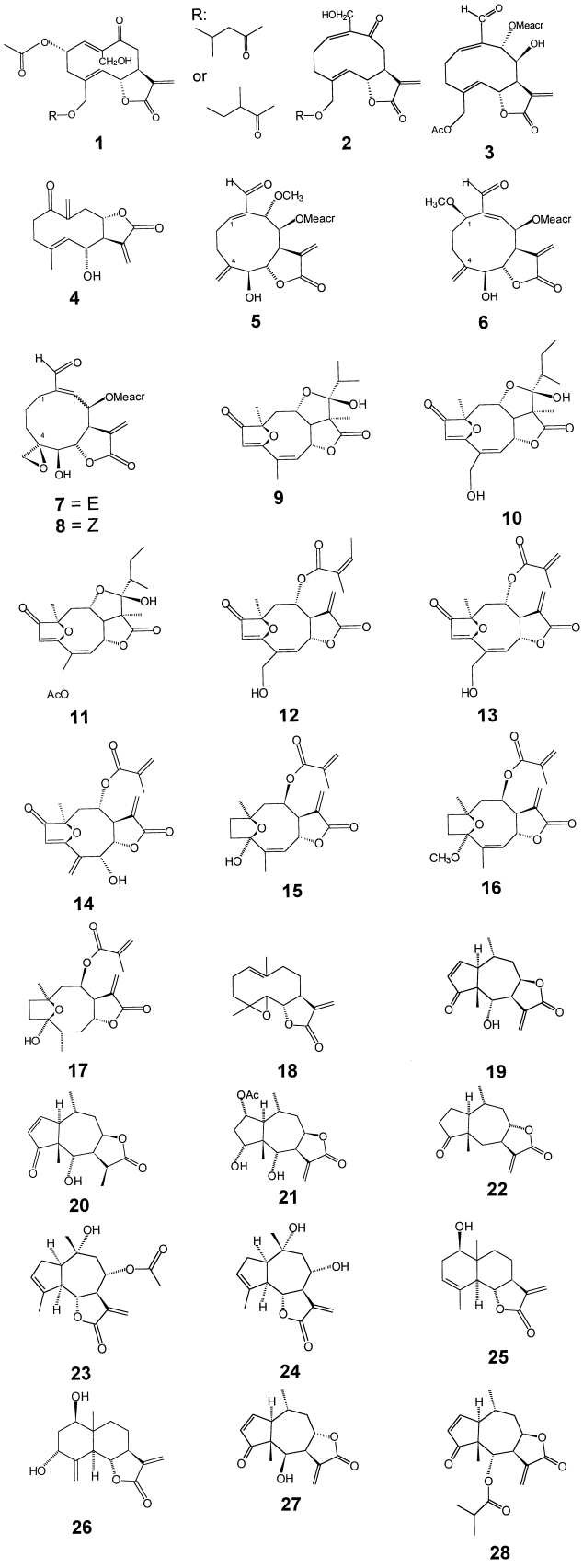

Figure 1. Structures of the investigated sesquiterpene lactones.

thereby inhibiting DNA binding. Inhibition of NF-κB DNA binding by monofunctional SLs requires alkylation of these cysteine residues by two SL molecules.

Results and Discussion

Sesquiterpene lactones are potent inhibitors of NF-κB activation

In order to investigate whether SLs **1**–**28** (see Figure 1 and Table 1) interfere with the activation of transcription factor NF-κB, Jurkat T cells were incubated with the respective SL at various concentrations for 1 h and subsequently stimulated with TNF-α for 1 h. Total protein extracts were prepared and analyzed for NF-κB DNA binding in an electrophoretic mobility shift assay (EMSA) (for example, see Figure 2). Stimulation with TNF-α induced one novel DNA binding activity in Jurkat T cells (for example, Fig. 2, lane 2). Antibody reactivity and competition assays identified this complex as a NF-κB p50/p65 heterodimer (data not shown[30]). With the exception of compound **9** all SLs prevented NF-κB induction. Different concentrations of compounds were however required for complete inhibition. None of the substances used showed any cytotoxic effects.

Inhibitory activity of different SLs and structure–activity relationships

The 28 investigated SLs can be divided into three activity groups: highly active inhibitors showing complete inhibition at concentrations (IC_{100}) between 5 and 20 μM (group 1), compounds with intermediate activity (IC_{100} ca. 50 μM, group 2) and less potent inhibitors (group 3) with IC_{100} values of 100 μM and above (see Table 2).

The most potent group 1 (**1**–**3**, **6**–**8**, **11**–**14**, **18**, **19**, **23**, **27** and **28**) comprises compounds of different skeletal types, namely pseudoguaianolides (**19**, **27** and **28**), guaianolides (**23**), germacrolides (**1** and **18**), heliangolides (**11**–**14**) melampolides (**2** and **3**) and 4,5-dihydrogermacranolides (**6**–**8**). Quite conspicuously, with three exceptions (**11**, **18** and **23**), these potent inhibitors, in addition to an α-methylene-γ-lactone group possess at least one further α,β- or α,β,γ,δ-unsaturated carbonyl group, and may thus be considered bifunctional Michael acceptors (alkylants). Some compounds, which possess an additional α,β-unsaturated acyl sidechain may even be considered trifunctional. Two compounds, **4** and **5** which also possess more than one potentially alkylating group appear in group 2 with intermediate activity (50 μM).

Table 1. List of the investigated sesquiterpene lactones and their origin

SL. no	Name	Origin/reference
1	mixture: 2-α-acetoxy-14-hydroxy-15-isovaleroyl-oxy-9-oxo-costunolide/2-α-acetoxy-14-hydroxy-15-(2-methyl-butyryloxy)-9-oxo-costunolide	*Mikania guaco*[a]
2	mixture: 14-hydroxy-15-isovaleroyloxy-9-oxo-melampolide/14-hydroxy-15-(2-methyl-butyryloxy)-9-oxo-melampolide	*M. guaco*[a]
3	15-acetoxy-9α-hydroxy-8β-methacryloyloxy-14-oxo-acanthospermolide	*Milleria quinqueflora*[18]
4	tamirin	*Tanacetum chiliophyllum*[19]
5	9-methoxy-miller-1(10)-*Z*-enolide	*M. quinqueflora*[20]
6	1-methoxy-miller-9*Z*-enolide	*M. quinqueflora*[20]
7	4β,15-epoxy-miller-9*E*-enolide	*M. quinqueflora*[18]
8	4β,15-epoxy-miller-9*Z*-enolide	*M. quinqueflora*[18]
9	eremantholide A	*Eremanthus eleagnus*[21]
10	15-hydroxy-eremantholide B	*Vanillomopsis arborea*[b]
11	15-acetoxy-eremantholide B	*V. arborea*[b]
12	centratherin	*Proteopsis furnensis*[22]
13	goiazensolide	*Eremanthus mattogrossensis*[23]
14	isogoiazensolide	*E. mattogrossensis*[23]
15	diversifolin	*Tithonia diversifolia*[24]
16	diversifolinmethylether	*T. diversifolia*[24]
17	tirotundin	*T. diversifolia*[24]
18	parthenolide	Aldrich Chemicals
19	helenalin	*Arnica chamissonis* ssp. *foliosa*[25]
20	11α,13-dihydrohelenalin	*A. chamissonis ssp. foliosa*[25]
21	chamissonolid	*A. chamissonis ssp. foliosa*[25]
22	2,3-dihydroaromaticin	*Arnica cordifolia*[26]
23	cumambrin A	*Tanacetum densum*[27]
24	cumambrin B	*T. densum*[27]
25	santamarin	*T. praeteritum*[28]
26	3-α-hydroxy-reynosin	*Tanacetum praeteritum*[28]
27	Mexicanin I	*Arnica acaulis*[29]
28	helenalin isobutyrate	*A. chamissonis* ssp. *foliosa*[25]

[a] P. Rüngeler and I. Merfort, unpublished.
[b] W. Vichnewski, unpublished.

Most SLs which only possess either a methylene lactone or a conjugated keto group fall into the least potent class of inhibitors (group 3), since they require inhibitory concentrations of about 100–200 μM. This lack of activity cannot be compensated by the presence of an α,β-unsaturated ester group. There are five notable exceptions from this observation: strongly active compounds **11**, **18** and **23** mentioned above, which belong to group 1, and two compounds (**15** and **22**) whose inhibitory concentrations lie in the intermediate range at 50 μM and thus belong to group 2.

Two of the monofunctional compounds, **10** and **11**, deserve separate mentioning. They differ from the completely inactive **9** only by an additional hydroxy or acetoxy group at C-4. However, these slight changes result in drastically lowered IC_{100}-values, 100 μM for compound **10** and 5 μM for compound **11**.

Although a detailed study of quantitative structure–activity relationships (QSAR) is certainly not possible on the basis of our data since the test system as currently applied does not allow a more exact quantification of the biological effect (i.e. measurement of dose–response curves), it is nonetheless possible to express the above mentioned relationship between the number of alkylating centers and activity in numerical form which shows its relevance and significance. Free and Wilson[31] developed a QSAR method that correlates biological activity with a set of variables indicating the presence or absence of particular structure elements, which was later refined by Fujita and Ban.[32] This method allows a description of the influence of structural features on activity in terms of a multilinear regression equation. In the case of our data set, the correlation coefficient R between the total number of potentially alkylating centres (NAC) and $\log(1/IC_{100})$ is 0.55 ($F=11$, $n=28$). NAC comprises the methylene lactone (ML), conjugated keto- or aldehyde (ENONE) and conjugated ester (ACYL) groups. When a multiple linear regression in the manner of a Free–Wilson QSAR analysis[31–33] is applied, using distinct variables for the three types of alkylating centers (i.e. assigning a value of 1 for the presence or 0 for the absence of the particular structure element), the resulting R value is increased to 0.66. The t-test P values for the three variables' regression coefficients are 0.04 (ML), 0.0008 (ENONE) and 0.91 (ACYL). These data clearly show that the ACYL variable does not significantly contribute to the correlation, which means that the conjugated acyl rest does not contribute significantly to the inhibitory activity. Consequently, reduction of the NAC variable to the sum of ML and ENONE, yielded a more significant correlation ($n=28$, $R=0.66$, $F=20$, $P=1.4\times10^{-4}$).

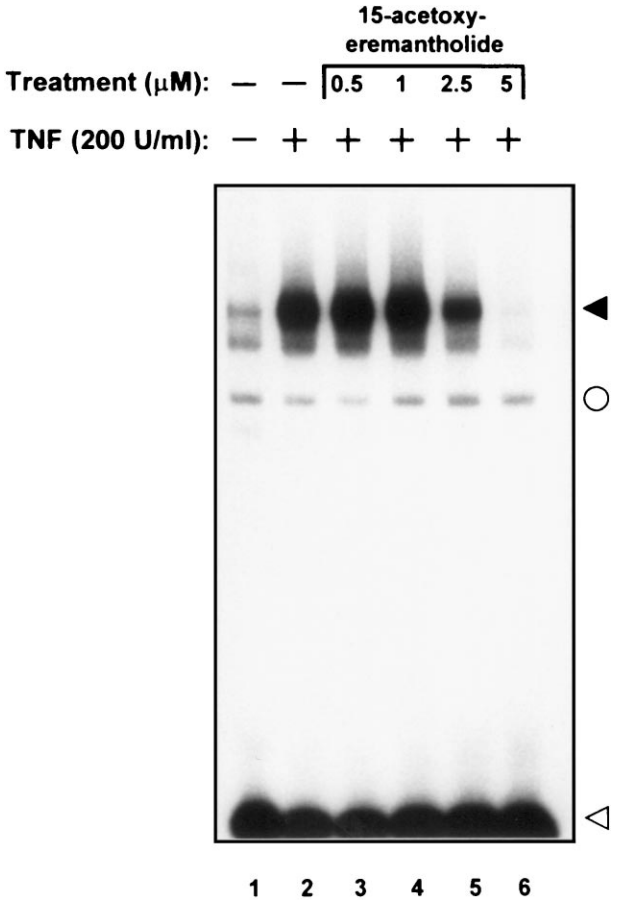

Figure 2. The effect of SL 11 on NF-κB DNA binding. Lane 1 shows unstimulated control cells, in lane 2 cells were treated with 200 U/mL TNF-α alone. In lanes 3–6 cells were pretreated for one hour with various concentrations of compound **11** and subsequently stimulated with TNF-α for 1 h. A filled arrowhead indicates the position of NF-κB DNA complexes. The open circle denotes a non-specific activity binding to the probe. The open arrowhead shows unbound oligonucleotide.

Table 2. Results of the NF-κB assay and log P values

SL	Inhibitory concentration (μM)	Log P
Group 1[a]		
1	12.5	2.3
2	12.5	2.4
3	5	1.9
6	20	2.0
7	5	1.9
8	10	1.8
11	5	3.5
12	5	2.0
13	20	1.8
14	10	1.8
18	20	2.3
19	10	1.5
23	20	2.2
27	20	1.5
28	20	2.3
Group 2[b]		
4	50	1.3
5	50	1.4
15	50	2.5
22	50	2.1
Group 3[c]		
9	>300	3.1
10	100	2.4
16	200	3.2
17	200	2.8
20	200	1.5
21	200	1.8
24	100	2.1
25	200	2.2
26	200	1.6

[a] Group 1: IC_{100}: 5–20 μM.
[b] Group 2: IC_{100}: 50 μM.
[c] Group 3: IC_{100}: ≥100 μM.

As expected, when reduced by the seven mentioned outliers (**4**, **5**, **11**, **15**, **18**, **22** and **23**), that is, bifunctional compounds with lower and monofunctional compounds with higher activity, the resulting linear regression $\log(1/IC_{100}) = 1.269\ NAC + 2.42$ describing the remaining 75% of the data set becomes highly significant with $R = 0.93$, $F = 121$ and $P_{(NAC)} = 1.1 \times 10^{-9}$, $P_{(y\text{-intercept})} = 9 \times 10^{-11}$; ($n = 21$). Taken together, these results clearly show the general dependence of NF-κB inhibition on the alkylant bifunctionality of SLs.

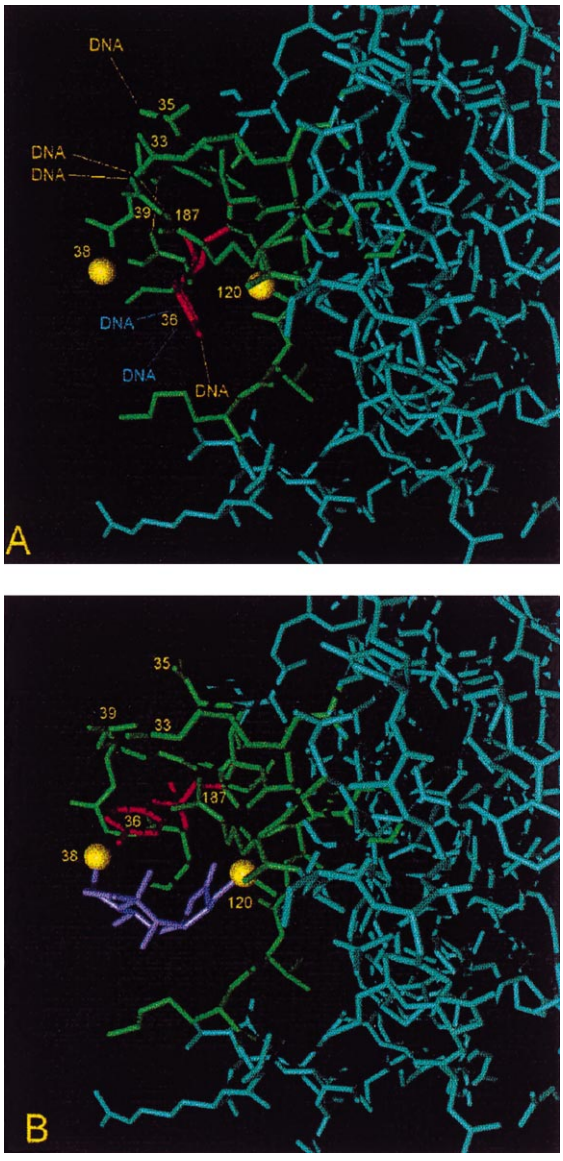

Figure 3. Changes in Protein tertiary structure induced by cross linkage of L1-Cys 38 and E'-Cys 120 of NF-κB/p65 by helenalin (**19**). A: Native protein X-ray structure[17] of NF-κB/p65 homodimer subunit A. B. Energy minimized structure after cross linkage of Cysteine residues by helenalin. Turquoise: Protein portion kept rigid during energy minimization. Green: Protein portion treated as flexible during energy minimization. Light blue: Sesquiterpene lactone molecule. Yellow spheres: Cysteine sulfur atoms. Red: Residue Tyr36. The other labelled residues Glu39, Arg33, Arg35 and Arg187 contribute to p65-DNA binding and recognition as indicated by yellow lines (hydrogen bonding) and light blue lines (van der Waals interactions with DNA).

We furthermore investigated the impact of lipophilicity (governing the penetration of drugs into the cell) on inhibitory activity. To this end we determined the logarithmic partition coefficient log P, which is commonly used in QSAR studies to express lipophilicity for each compound. The log P values for our set of compounds all lie in a range between 1.3 and 3.5 (see Table 2). No correlation between reactivity towards NF-κB and lipophilicity could be observed. SLs with a similar log P, for example, compounds **9** (log P 3.1) and **11** (log P 3.5) as well as **23** (log P 2.2) and **24** (log P 2.1) show significant differences in their ability to inhibit NF-κB (see Table 2). Furthermore, log P does not significantly improve the above mentioned correlation between NAC and $\log(1/IC_{100})$ when added to the regression as a second independent variable ($n = 21$, $R = 0.94$, $F = 63$, $P_{(NAC)} = 1.1 \times 10^{-8}$, $P_{(\log P)} = 0.23$). It is therefore unlikely that lipophilicity influences NF-κB inhibitory activity in this set of compounds.

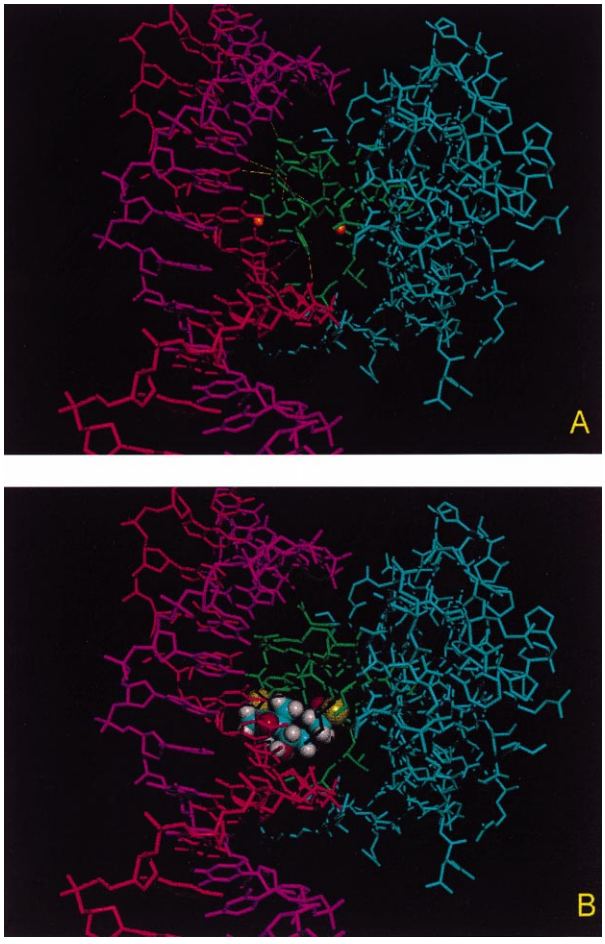

Figure 4. Cross linkage of L1-Cys and E'-Cys of NF-κB/p65 by helenalin (**19**) directly hinders DNA binding. Unchanged NF-κB/p65 and DNA X-ray structure.[17] Some of the crucial interactions via hydrogen bonds (yellow lines) and van der Waals contacts (light-blue lines) are marked. B. Overlay of the cross-linked protein structure with the DNA structure from A. Some atoms of helenalin occupy space that would be reserved for atoms of the DNA. Turquoise: Protein region kept rigid during energy minimization. Green: Protein region treated as flexible during energy minimization. Red and purple: DNA strands.

Proposed molecular mechanism of action of NF-κB inhibition by sesquiterpene lactones

It has been demonstrated that DNA binding of NF-κB is sensitive to alkylation by *N*-ethylmaleimide and other chemical modifications.[34,35] Modification of a free cysteine residue in the vicinity of the DNA binding loop 1 (L1) is thought responsible for this effect.[35] This was shown with the p50 homodimer. In a previous study we have demonstrated, that helenalin (**19**) inhibits DNA binding of the p65 homodimer of NF-κB at low concentrations while binding of the p50 homodimer is unaffected by the drug, even in higher concentrations.[13]

In order to find an explanation for this p65 selectivity and for the observed correlation of high activity with alkylant bifunctionality we undertook a molecular modelling study. We used the published X-ray structures of both NF-κB subunits, p50 and p65, as the basis for our models.[17,36] In both the p50/p50 and p65/p65 homodimers, a cysteine residue (L1-Cys, position 59 in p50, position 38 in p65) participates in DNA binding by forming a hydrogen bond with the phosphate-sugar backbone of the κB-DNA motif.[17,36] Several amino acid residues in the immediate vicinity of L1-Cys, Arg 33, Arg 35, Tyr 36, Glu 39, and Arg 187 (residue numbering for p65, according to ref 17) are known to be essential for DNA recognition and binding.[17]

A very conspicuous difference between the two proteins in the vicinity of this L1-Cys is that His 141 in the nearby E' region of p50 is replaced by another free cysteine in the corresponding position 120 of p65. The sulfur atom of this second cysteine (E′-Cys, Cys 120) is placed at a distance of only 8 Å from that of the L1-Cys. This distance is small enough to allow alkylation of both sulfur atoms by a single bifunctional SL molecule such as helenalin. This creates a cross link between Cys 38 and Cys 120 in the p65 molecule. The p65 X-ray structure shows a gap region between these Cys residues, which is large enough to hold a sesquiterpene lactone molecule. The gap is empty except for the phenol ring of Tyr 36 whose interactions with the DNA's backbone and with two Thymin residues are essential for DNA binding. If p65 were alkylated at the two cysteine residues (Cys 38 and Cys 120) by a SL, the Tyr 36/DNA interactions would become essentially impossible. The spatial arrangement of amino acids Arg 33, Arg 35, Tyr 36, Cys 38, Glu 39 and Arg 187 is crucial for the homodimer's specific DNA binding. Alteration of the geometry in this small region would dramatically affect the capability of p65 to recognize and bind to the κB-DNA motif.

We generated molecular models of p65 with both Cys residues cross linked by a covalently bound helenalin molecule in order to examine the geometric changes that would be induced by this reaction. Figure 3 shows the spatial arrangement in this region of p65 in the unaltered protein as observed in the X-ray structure (A), and after insertion of a helenalin molecule connected to the Cys-sulfurs and subsequent force field energy minimization (B). As expected, dramatic changes in the positions of the amino acid side chains of Tyr 36 (marked in red in Figure 3) and the other mentioned residues occur. It is obvious that a p65 molecule altered in this way would no longer possess the reported binding specificity.[17] Moreover, an overlay of the alkylated p65 model with the original X-ray structure of p65 bound to DNA (Fig. 4) shows that the SL molecule extends into a region that would be occupied by atoms of the DNA's sugar/phosphate backbone. Therefore, alkylation directly hinders DNA binding in this region.

Consequently, we created analogous models of all the bifunctionally alkylating SLs used in this study. Figure 5 shows a superposition of all these models viewed from the same angle as depicted for helenalin in Figure 3. All the molecules are capable of inducing largely the same changes in amino acid geometry. All SLs in this model extend into the region otherwise reserved for DNA.

The p50 subunit, which possesses only the L1-cys residue (Cys 59) in this region can only be alkylated at this position. In this case, the SL molecule after binding could more easily be oriented in such a way that it does not interfere with the protein's tertiary structure or occupy positions reserved for atoms of the DNA.

As shown above, SLs containing only one potentially alkylating center (group 3) show much lower NF-κB inhibitory activity. The IC_{100} is increased by an order of magnitude compared to the bifunctional alkylants. We therefore also created molecular models of the same region of p65 alkylated at the L1-Cys by monofunctional SLs. Figure 6, as an example, shows a chamissonolid (**21**) molecule bound to L1-Cys (B) in comparison with the unaltered structure of p65 bound to DNA (A). It can be seen that no significant changes in the orientation of amino acid sidechains are induced. The SL molecule is attached to the protein backbone via four rotatable bonds and can thus easily be oriented in such a way that it does not cause changes in the orientation of amino acid sidechains or interfere with atoms of the DNA. Even though formation of a hydrogen bond between the

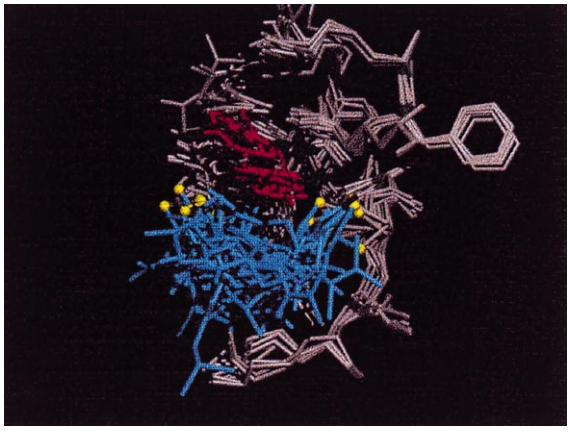

Figure 5. Overlayed structures of bifunctional sesquiterpene lactone adducts with NF-κB/p65. Light grey: NF-κB/p65 protein portion included in the energy minimization; Red: Sidechain of Tyrosin residue 36; Light blue: Sesquiterpene lactones; Yellow spheres: Sulfur atoms of residues L1-Cys 38 (left) and E'-Cys 120 (right).

S–H of L1-Cys and the DNA would no longer be possible, the overall structure, especially the orientation of the crucial residues Arg 33, Arg 35, Tyr 36, Glu 39, and Arg 187 is unchanged and DNA binding would be less dramatically affected than in a p65 molecule with the two Cys residues cross linked by a bifunctional SL.

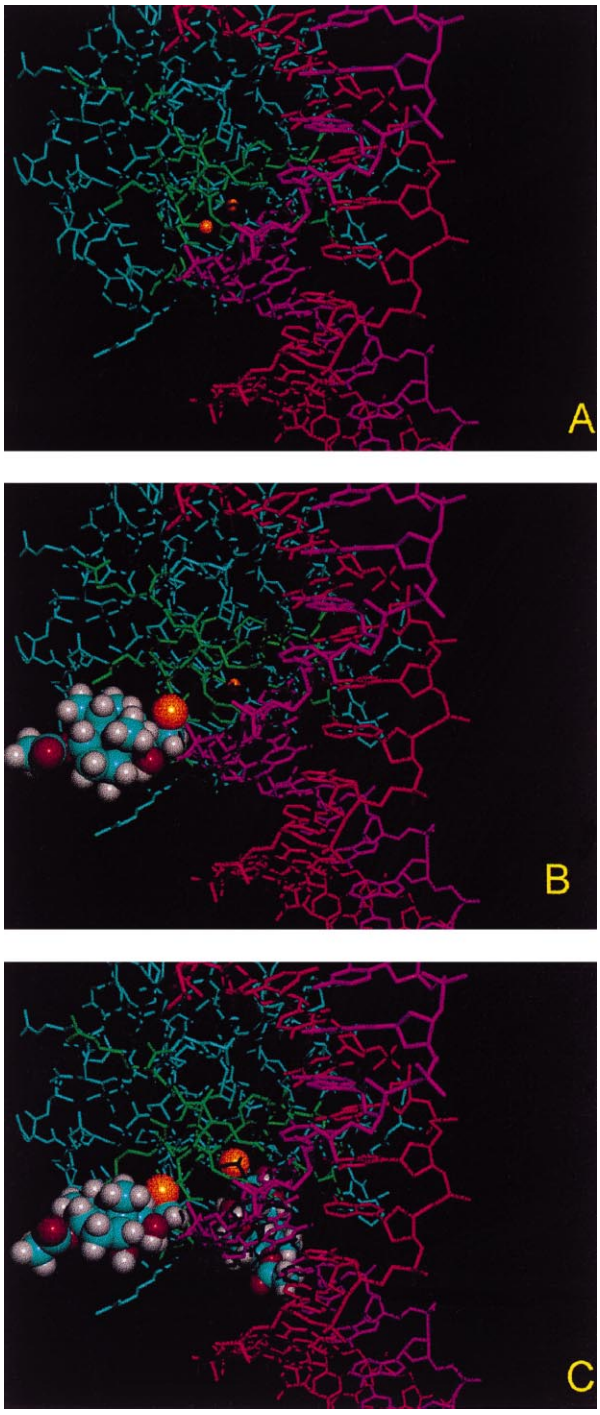

Figure 6. Effects of mono- and bifunctional alkylation by monofunctional sesquiterpene lactone chamissonolide (**21**) on DNA binding of NF-κB/p65. A. Unchanged NF-κB/p65 protein and DNA X-ray structure.[17] B. L1-Cys alkylated by a single chamissonolide molecule. C. L1-Cys and E'-Cys alkylated by two chamissonolide molecules. Turquoise: Protein region kept rigid during energy minimization. Green: Protein region treated as flexible during energy minimization. Red and purple: DNA strands.

If, however, the E'-Cys (Cys 120) is also alkylated by a *second* chamissonolide molecule (Fig. 6C), more dramatic changes in protein structure are observed. The second SL molecule in this case would extend into the DNA region. Since reaction with the E'-Cys is sterically more hindered than reaction with the L1-Cys, for thermodynamic reasons much higher concentrations of the SL will be required for alkylation at both positions. This explains the higher IC_{100} required of monofunctional compounds.

Conclusions

The model presented here provides a general molecular mechanism for NF-κB inhibition by SLs. It is in agreement with both our basic experimental observations, the pronounced correlation of high activity with bifunctionality *and* the selectivity towards p65 observed with helenalin.[13] Deviations from this model, such as the high activity of some of the monofunctional compounds and the low activity of a few bifunctional ones may be caused by additional more specific non bonding interactions with the protein. It is, for example quite conspicuous, that in two cases (compounds **11** and **23**) *O*-acetyl derivatives of monofunctional alkylants are much more active than the parent alcohols (compounds **10** and **24**, respectively). This effect may be due to the capability to accept a hydrogen bond in the vicinity of the alkylating site. Such interactions, however, cannot be sufficiently explained with our present knowledge. Moreover, a more precise measurement of activity differences, which we are currently attempting, will allow more detailed QSAR studies elucidating the structural factors that modulate the activity apart from alkylant functionality.

In this respect, monofunctional SLs with potent NF-κB inhibitory activity will be of special interest, since monofunctional alkylants can be expected to possess less unwanted effects such as cytotoxicity (e.g. ref 37) or contact dermatitis.[38]

Although we are not as yet able to provide a *direct* chemical proof that NF-κB inhibition by SLs is caused by alkylation at the mentioned cysteines in p65, the underlying chemical reaction has been shown to occur with low molecular weight thiols in many instances (e.g. refs 2–4). It is known that SLs' enzyme inhibitory activity is usually associated with the presence of free cysteine residues. At the same time, as mentioned above, NF-κB inhibition by an alkylant of completely different structure has been demonstrated.[34,35] These facts make the presented model a very plausible one.

Experimental

Abbreviations

BSA: bovine serum albumen; cpm: counts per minute; DTT: dithiothreitol; EDTA: ethylenediaminetetraacetic acid; EGTA: ethylene glycol-bis(β-aminoethyl ether)

N,*N*,*N*′,*N*′ tetraacetic acid; HEPES: (N-[2-hydroxyethyl] piperazine-*N*′-[2-ethanesulfonic acid]); NP-40: (nonylphenoxy)-(polyethoxy)-ethanol; PBS: phosphate-buffered saline; PMSF: phenylmethylsulfonyl fluoride; poly (dI-dC): polydeoxyinosinicdeoxycytidylic acid, double-stranded alternating copolymer; R: linear correlation coefficient; F = *F*-test value, representing a measure for the significance of a linear regression; P = *t*-test *P* value for regression coefficients, representing a measure for the significance of an independent variable in a multivariate linear regression, small values indicating high significance.

Cell culture

Jurkat T cells were maintained in RPMI 1640 supplemented with 10% fetal calf serum and 100 IU/mL penicillin and 100 μg/mL streptomycin (all Gibco-BRL).

Test compounds

The 28 SLs were isolated from different species as listed in Table 1.[18–29] 10 mM stock solutions were prepared in DMSO for the NF-κB assays.

Electrophoretic mobility shift assays

Total cell extracts from Jurkat T cells were prepared using a high-salt detergent buffer (Totex = 20 mM HEPES, pH 7.9, 350 mM NaCl, 20% (v/v) glycerol, 1% (w/v) NP-40, 1 mM $MgCl_2$, 0.5 mM EDTA, 0.1 mM EGTA, 0.5 mM DTT, 0.1% PMSF, 1% aprotinin). Cells were harvested by centrifugation, washed once in icecold PBS (Sigma) and resuspended in 4 cell volumes of Totex buffer. The cell lysate was incubated on ice for 30 min, then centrifuged for 5 min at 13,000 rpm at 4°C. The protein content of the supernatant was determined and equal amounts of protein (10–20 μg) added to a reaction mixture containing 20 μg BSA (Sigma), 2 μg poly (dI-dC) (Boehringer), 2 μL buffer D+ (20 mM HEPES, pH 7.9; 20% glycerol, 100 mM KCl, 0.5 mM EDTA, 0.25% NP-40, 2 mM DTT, 0.1% PMSF), 4 μL buffer F (20% Ficoll 400, 100 mM HEPES, 300 mM KCl, 10 mM DTT, 0.1% PMSF) and 100,000 cpm (Cerenkov) of a ^{32}P-labeled oligonucleotide, made up to a final volume of 20 μL with distilled water. Samples were incubated at room temperature for 25 min NF-κB oligonucleotide (Promega) was labeled using γ-[^{32}P]-ATP (3000 Ci/mmol; Amersham) and a T4 polynucleotide kinase (Promega).

NF-κB DNA binding assay

Jurkat T cells were incubated with various concentrations of the SLs for 1 h and subsequently stimulated with TNF-α for 1 h. Total protein extracts were prepared and analyzed for NF-κB DNA binding activity in an electrophoretic mobility shift assay (EMSA). All experiments were carried out three times.

Partition coefficient (*n*-octanol/water); HPLC-method

The partition coefficients of the different compounds were determined using an HPLC method following the OECD guideline for testing of chemicals No. 117 (adopted 30.03.1989).[39] HPLC was performed on an analytical RP-18 column (Bischoff ODS-Hypersil 5 μm; 125×4.6 mm) with mixtures of HPLC-grade methanol and destilled water (30, 40, or 50% methanol). A diode array detector was used. The dead time t_0 was measured with thiourea (Fluka), which leaves the column unretained. As reference compounds we used 2-butanone (log P: 0.3; Merck), benzyl alcohol (log P: 1.1; Roth), benzonitrile (log P: 1.6; Fluka), acetophenone (log P: 1.7; Fluka), cinnamic alcohol (log P: 1.9; Roth), anisole (log P: 2.1; Merck), methyl benzoate (log P: 2,1; Fluka), 1,1,1-trichloroethane (log P: 2,4; Fluka), ethyl benzoate (log P: 2.6; Fluka), allyl phenyl ether (log P: 2.9; Fluka), thymol (log P: 3.3; Merck) and naphthalene (log P: 3.6; Aldrich). The partition coefficient is deduced from the capacity factor k, which is derived from the following formula:

$$k = t_R - t_0/t_0$$

where t_R is the retention time of the substance. The logarithms of the capacity factors of the reference compounds, log k, are calculated and plotted as a function of log P. Log P of the SLs is obtained by measuring the retention times and interpolating the calculated capacity factors on the calibration graph. For each compound retention times were measured twice. The calibration was performed once daily.

Linear regression analysis

Regression analysis to investigate the correlation of the activity data with structure elements and log P values was carried out using the statistical analysis tool implemented with Microsoft Excel97®.

Molecular modelling

All molecular models were created using the Molecular Modelling package Hyperchem® (versions 4.5 and 5.0). The protein structures were obtained from the Brookhaven Protein Data Bank and converted to Hyperchem input. Energy minimizations were performed with Hyperchem's force field MM+ which is a modification of N.L. Allinger's MM2[40] using the Polak–Ribiere minimization algorithm. In calculations of the protein and of protein–SL-conjugates, a switched cutoff (inner radius = 10 Å, outer radius = 14 Å) was applied for the nonbonded electrostatic interactions.

Modelling of SLs

Low-energy conformations of the SLs were generated using the conformational search option as implemented with ChemPlus®, v. 1.6. All starting structures (3-D models created with Hyperchem or from X-ray coordinates from the Cambridge Crystallographic Data Bank) (compounds **18** and **22**) were initially minimized to an RMS gradient < 0.01 kcal mol^{-1} Å^{-1}. All rotatable cyclic bonds were included as variable torsions and allowed to be changed simultaneously. The search was performed applying a usage directed search method and standard settings for duplication tests. A search run was

terminated after energy minimization of 2500 unique starting geometries.

The conformers with the lowest energy were used for subsequent modelling of the protein adducts with the exception of helenalin (**19**). Here, the conformer (TC7) which has been shown to be the most stable form in the conformational equilibrium as found in aq soln[41] and, even more importantly, was also demonstrated to represent the conformation of helenalin's mono- and bis-adducts with the tripeptide glutathione,[4] was used.

Acyl side chains were not included in the conformational searches since they would cause a vast increase in computation time and in the number of distinct conformations found. Since these side chains are more or less freely rotatable, they can easily adopt an energetically favorable orientation within the conjugate SL–protein models. They were therefore added manually to the most favorable SL-conformers and the resulting models were energy minimized to an RMS gradient as above to be used as starting geometries for the protein conjugates.

SL-p65 conjugates

Since only part of the p65 protein was of interest, we undertook the following modifications to the original X-ray structure.

From p65 subunit A in the input file PDB1RAM,[17] a spheric fragment of all amino acids possessing atoms within a radius of 25.0 Å distance from the sulfur atom of L1-Cys 38 was chosen to be included in the models. All other atoms were deleted. The SL models were manually inserted into this protein fragment and their electrophilic centers connected to the sulfur atoms. In the case of bifunctional SLs, the more exposed L1-Cys was generally connected with the center expected to possess higher reactivity (higher carbonyl activity), that is, the β- or δ-position in conjugated keto- or aldehyde groups, while the exomethylene lactone group was connected to E′-Cys. After the necessary structural changes (deletion of sulfhydryl-hydrogens, replacement of conjugated double bonds by single bonds, addition of H-atoms to the α-position and recalculation of atom types) in each composite model a spheric portion of all amino acids possessing atoms within a radius of 10.0 Å distance from the sulfur of L1-Cys was energy minimized together with the inserted SL molecule in the MM+ force field to an RMS gradient <0.1 kcal mol^{-1} Å^{-1}. The remainder of the 25 Å sphere was not included in the energy minimization but was allowed to interact with the portion under minimization, applying the above mentioned cutoff conditions.

Models of monofunctional SLs were generated in the same way attaching the SL molecule to the L1-Cys sulfur and manually rotating it into a position with minimum interaction with the protein atoms, followed by energy minimization as above.

Graphic representations of the molecular models as presented in Figures 3–6 were generated using the program POVRay®.

Acknowledgements

We are grateful to the Albert-Ludwigs-Universität for a grant and to the Wissenschaftliche Gesellschaft, Freiburg for financial support.

References

1. Seaman, F. C. *Bot. Rev.* **1982**, *48*, 121.
2. Picman, A. K. *Biochem. Syst. Ecol.* **1986**, *14*, 255.
3. Kupchan, S. M.; Fessler, D. C.; Eakin, M. A.; Giacobbe, T. J. *Science* **1970**, *168*, 376.
4. Schmidt, T. J. *Bioorg. Med. Chem.* **1997**, *5*, 645.
5. Kupchan, S. M.; Eakin, M. A.; Thomas, A. M. *J. Med. Chem.* **1971**, *14*, 1147.
6. Lee, K.-H.; Ibuka, T.; Wu, R.-Y.; Geissman, T. A. *Phytochemistry* **1977**, *16*, 1177.
7. Marles, R. J.; Pazos-Sanou, L.; Compadre, C. M.; Pezzuto, J. M.; Bloszyk, E.; Arnason, J. T. In *Phytochemistry of Medicinal Plants*, Arnason, J. T., Mata, R., Romeo, J. T., Eds., Plenum: New York, 1995, p. 333.
8. Snyder, G. H.; Cennerazzo, M. J.; Karalis, A. J.; Field, D. *Biochemistry* **1981**, *20*, 6509.
9. Hall, I. H.; Starnes, C. O.; Lee, K.-H.; Waddell, T. G. *J. Pharm. Sci.* **1980**, *69*, 537.
10. Schröder, H.; Lösche, W.; Strobach, H.; Leven, W.; Willuhn, G.; Till, U.; Schröer, K. *Throm. Res.* **1990**, *57*, 839.
11. Lyß, G.; Schmidt, T. J.; Merfort, I.; Pahl, H. L. *Biol. Chem.* **1997**, *378*, 951.
12. Rüngeler, P.; Lyß, G.; Castro, V.; Mora, G.; Pahl, H. L.; Merfort, I. *Planta Med.* **1998**, *64*, 588.
13. Lyß, G.; Knorre, A.; Schmidt, T. J.; Pahl, H. L.; Merfort, I. *J. Biol. Chem.* **1998**, *273*, 33508.
14. Baeuerle, P. A.; Henkel, T. *Annu. Rev. Immunol.* **1994**, *12*, 141.
15. Baeuerle, P. A.; Baltimore, D. *Cell* **1996**, *87*, 13.
16. May, M. J.; Ghosh, S. *Immunology Today* **1998**, *19*, 80.
17. Chen, Y.-Q.; Ghosh, S.; Ghosh, G. *Nat. Struct. Biol.* **1998**, *5*, 67.
18. Jakupovic, J.; Castro, V.; Bohlmann, F. *Phytochemistry* **1987**, *26*, 2011.
19. Gören, N.; Tahtasakal, E. *Phytochemistry* **1993**, *34*, 1071.
20. Castro, V.; Rüngeler, P.; Murillo, R.; Hernandez, E.; Mora, G.; Pahl, H. L.; Merfort, I. in press.
21. Le Quesne, P. W.; Leverey, S. B.; Menachery, M. D.; Brennan, T. F.; Raffauf, R. F. *J. Chem. Soc. Perkin Trans 1* **1978**, 1572.
22. Vichnewski, W.; Semir, J.; Leitsao Filho, H. F.; Nakashima, C.; Lunardello, M. A.; Gutierrez, A. B.; Herz, W. *Rev. Latinoam. Quim.* **1990**, *21*, 28.
23. Lunardello, M. A.; Tomaz, J. C.; Vichnewski, W.; Lopes, J. L. C. *J. Braz. Chem. Soc.* **1995**, *6*, 307.
24. Schuster, A.; Stokes, S.; Papastergiou, F.; Castro, V.; Poveda, L.; Jakupovic, J. *Phytochemistry* **1992**, *31*, 3139.
25. Willuhn, G.; Kresken, J.; Leven, W. *Planta Med.* **1990**, *56*, 111.
26. Merfort, I.; Wendisch, D. *Phytochemistry* **1993**, *34*, 1436.
27. Gören, N.; Bozok-Johansson, C.; Jakupovic, J.; Lin, L.-J.; Shieh, H.-L.; Cordell, G. A.; Celik, N. *Phytochemistry* **1992**, *31*, 101.
28. Gören, N. *Phytochemistry* **1995**, *38*, 1261.
29. Leven, W. Ph.D. thesis, University of Düsseldorf, 1988.
30. Pahl, H. L.; Baeuerle, P. A. *EMBO J.* **1995**, *14*, 2580.
31. Free, S. M.; Wilson, J. W. *J. Med. Chem.* **1964**, *7*, 395.
32. Fujita, T.; Ban, T. *J. Med. Chem.* **1971**, *14*, 148.
33. Seydel, J. K., Schaper, K.-J. *Chemische Struktur und biologische Aktivität von Wirkstoffen. Methoden der quantitativen Struktur-Wirkungs-Analyse*; Verlag Chemie: Weinheim, New York, 1979.
34. Toledano, M. B.; Leonard, W. J. *Proc. Natl. Acad. Sci. USA* **1991**, *88*, 4328.

35. Mitomo, K.; Nakayama, K.; Fujimoto, K.; Sun, X.; Seki, S.; Yamamoto, K. *Gene* **1994**, *145*, 197.
36. Ghosh, G.; Van Duyne, G.; Ghosh, S.; Sigler, P. B. *Nature* **1995**, *373*, 303.
37. Beekman, A. C.; Woerdenbag, H. J.; Van Uden, W.; Pras, N.; Konings, A. W. T.; Wikström, H. V.; Schmidt, T. J. *J. Nat. Prod.* **1997**, *60*, 252.
38. Hausen, B. M., Vieluf, I. K. *Allergiepflanzen, Pflanzenallergene*. Ecomed Verlagsgesellschaft Landsberg: München, 1997.
39. OECD guideline for testing of chemicals No. 117 (adopted 30.03.1989).
40. Allinger, N. L. *J. Am. Chem. Soc.* **1977**, *99*, 8127.
41. Schmidt, T. J. *J. Mol. Struct.* **1996**, *385*, 99.